Supporting Information for

Molecule stapling-assisted fabrication of high-quality $CsPbI_2Br$ films for efficient and stable photovoltaic modules

Ruihao Chen[a,b,c#*], Jieru Du[a#], Xuan Zheng[d#], Li Yuan[a], Yuyao Yang[a], Yang Yang[a], Feiming Li[d] and Hongqiang Wang[a*]

[a]School of Materials Science and Engineering, State Key Laboratory of Solidification Processing, Center for Nano Energy Materials, Northwestern Polytechnical University, Xi'an 710072, China

[b]Chongqing Innovation Center, Northwestern Polytechnical University, Chongqing, 401135, China

[c]Research & Development Institute of Northwestern Polytechnical University in Shenzhen, Shenzhen, 518063, China

[d]College of Chemistry, Chemical Engineering and Environment, Minnan Normal University, Zhangzhou, 363000, P.R. China

Corresponding Authors:

*E-mail: rhchen@nwpu.edu.cn; hongqiang.wang@nwpu.edu.cn

[#]These authors contributed equally to this work.

Materials: Chlorobenzene (CB), CsI and $PbBr_2$ were purchased from Alfa Aesar. Cesium hydroxide (CsOH, 50wt% in water), cesium bromide (CsBr, 98%), perfluoroglutaric acid ($H_2C_4F_4O_4$, 98%), perfluorosuccinic acid ($H_2C_5F_6O_4$, 97%) and perfluoroadipic acid ($H_2C_6F_8O_4$, 98%) was purchased from Aladdin (Shanghai, China). Ethanol, acetonitrile, dimethyl sulfoxide (DMSO), *N,N*-dimethylformamide (DMF) and isopropanol (IPA) were purchased from Sinopharm Chemical Regent Co., Ltd. PbI_2, Spiro-OMeTAD, ITO and FTO glass (NSG, Tec-7) were purchased from Advanced Election Technology Co., Ltd..

Synthesis of cesium hexafluoroglutarate ($C_5F_6O_4Cs_2$) and other cesium perfluorodioates salts: $C_5F_6O_4Cs_2$ was synthesized through $H_2C_5F_6O_4$ (1.2 g) in 10 mL isopropanol mixed with CsOH aqueous solution (800 μL) at 60 °C with continue stirring. And then the above mixture was crystallized at room temperature and purified several times by anhydrous ether. Finally, the product was obtained by vacuum-drying at 60 °C overnight. The synthesis of $C_4F_4O_4Cs_2$ and $C_6F_8O_4Cs_2$ were the same as the synthesis of $C_5F_6O_4Cs_2$.

Solar Cell Fabrications: A compact SnO_2 electron transport layer (ETL) on FTO or ITO was prepared by blade-coating a SnO_2 colloidal dispersion.[1] The $CsPbI_2Br$ precursor solution including 277 mg PbI_2, 220 mg $PbBr_2$, 312 mg CsI, 800 μL DMSO and 200 μL DMF, and then the above solution was kept at 70 °C with continue stirring. The solution (40 μL) was dropped and spun on the SnO_2/FTO or SnO_2/ITO film at 2500 rpm for 30 s, and then the as-prepared film was first heat-treated at 45 °C for 4 min and annealed again at 170 °C for 10 min. For depositing the Cs-HFG perovskite layer, 1 mg, 1.5 mg or 2.0 mg $C_5F_6O_4Cs_2$ was added in above $CsPbI_2Br$ solution (1 mL), and the fabrication of films was consistent with above control case. Else cesium perfluorodioate salts were optimized and added into the $CsPbI_2Br$ precursors, which is consistent with control case. After preparation of $CsPbI_2Br$ film, conventional Spiro-OMeTAD was used as the hole transport layer (HTL).[2] The fabrication process of P3HT HTL was accorded to the previous work.[3] Finally, 60 nm of Au was prepared via thermal evaporation. The active area was defined by a 0.12-cm^2 mask. The 16-cm^2 (8-cm^2 active area) PSC module were blade-coating fabricated referring to the previous work.[1, 4]

DFT calculation: The first-principles DFT calculation method was adopted to calculate the binding energy of different carboxylate ligands absorbed on the surface of $CsPbI_3$ crystal by CP2K 8.2 software package.[5] The Perdew-Burke-Ernzerhof (PBE) functional in conjunction with Goedecker-Teter-Hutter (GTH) pseudopotential and double-zeta GTH-MOLOPT basis set was employed,[6-8] and a 520 Ry cut-off energy was used. A (3*3) seven-slab model of (001) surface with a vacuum region of 20 Å was constructed to perform these calculations. The periodic boundary condition in the XY directions and a *Γ*-only *k*-point grid were considered due to the sufficient size of this model. The DFT-D3BJ method was also adopted to better describe the van der Waals

interactions.[9-10] During these geometry optimizations, the ligand molecule was placed near the surface and the top five atomic layers were fully relaxed, while the bottom two layers were fixed. In addition, the default convergence thresholds of force and geometry change, and an energy convergence criterion of $3*10^{-6}$ Hartree were used.

Based on these optimized structures, the binding energy of each carboxylate ligand ($\Delta E_{binding}$) was calculated as follows:

$$\Delta E_{binding} = E_{ligand/surface} - E_{surface} - E_{ligand}$$

Wherein, $E_{surface}$, E_{ligand}, and $E_{ligand/surface}$ are the energies of the (001) surface, ligand molecule, and the surface with ligand, respectively.

Characterizations: The *J-V* characteristics of PSCs were analyzed on a solar simulator (Newport, Class 3A, 84023A) under the AM 1.5G standard light (100 mW cm^{-2}) equipped with a Keithley 2400 source meter. The IPCE spectra were measured on an IPCE system (Newport) equipped with a Xenon lamp (66920, Newport, 300 W xenon lamp), a monochromator (Cornerstone 260, Newport) and a multimeter (Keithley 2400). The system was calibrated with the certified Si-reference cell. The perovskite films were analyzed on an X-ray diffractometer (Rigaku, SmartLab-SE) with a Cu *K*α radiation source. Surface and cross-sectional morphologies and EDS mapping of the perovskite films or devices were measured on a field-emission scanning electron microscope (SEM) (ZEISS, Sigma). The UV−vis spectra were recorded on a UV-2550 UV-vis spectrophotometer. IR spectra were collected on an infrared spectrometer instrument (Thermo Fisher, Nicolet iS50). The steady and time-resolved PL spectra were measured using an FLS980 (Edinburgh) fluorescence spectrometer excited by a 377.6 nm pulsed laser.

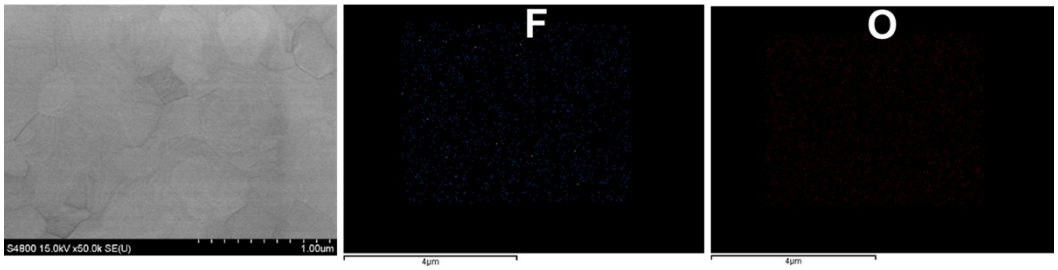

Figure S1. Top-view SEM image and EDS mapping of F and O elements of the Cs-HFG perovskite film.

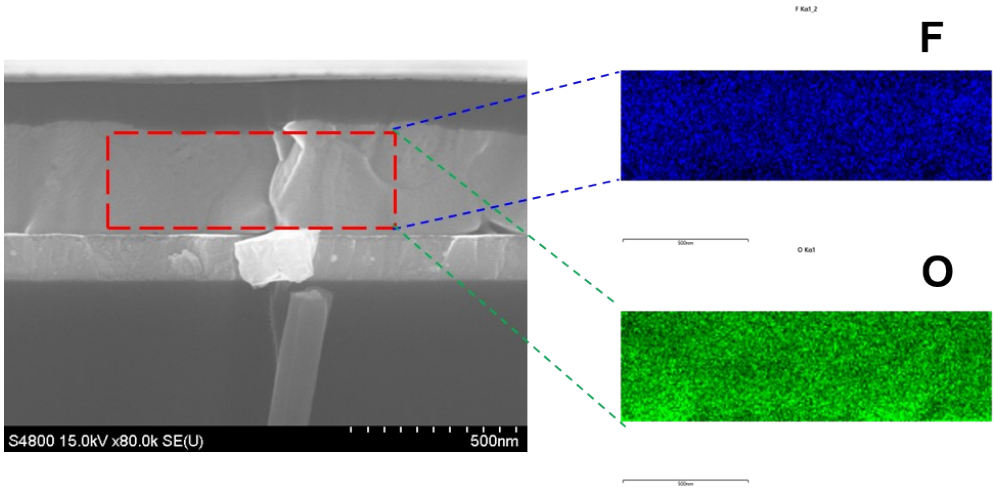

Figure S2. Cross sectional SEM image and EDS mapping of F and O elements of the Cs-HFG device.

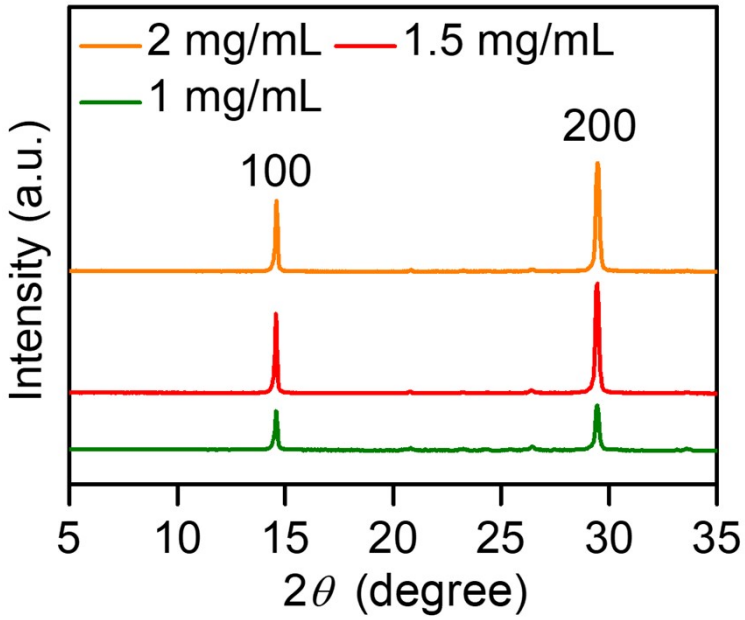

Figure S3. XRD patterns of the perovskite films with $C_5F_6O_4Cs_2$ in different concentrations.

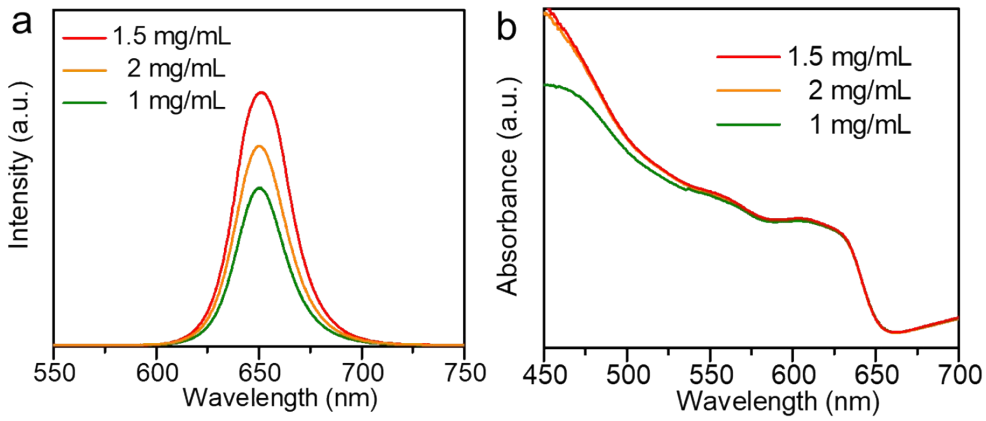

Figure S4. (a) PL and (b) UV-vis spectra of the perovskite films with $C_5F_6O_4Cs_2$ in different concentrations.

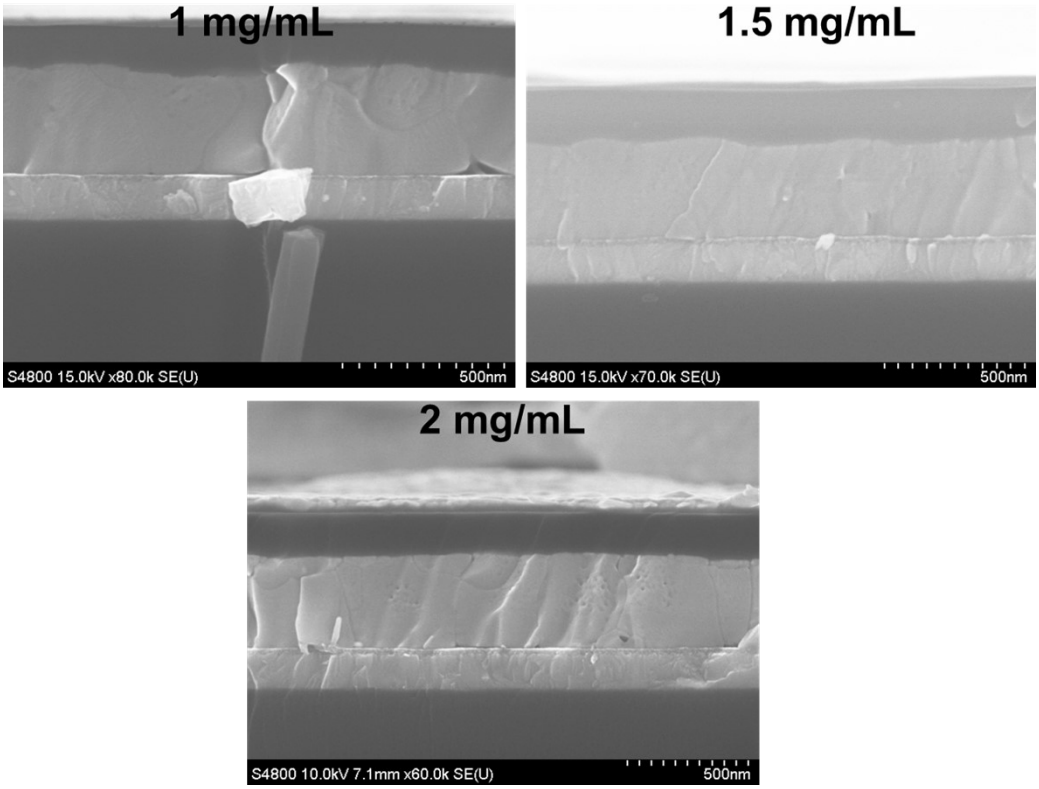

Figure S5. Cross sectional SEM images of the devices with $C_5F_6O_4Cs_2$ in different concentrations.

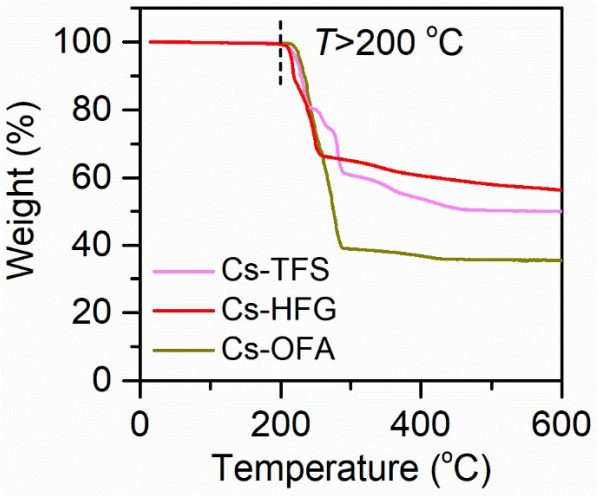

Figure S6. Thermogravimetric (TG) analysis of cesium-based TFS, HFG and OFA powders.

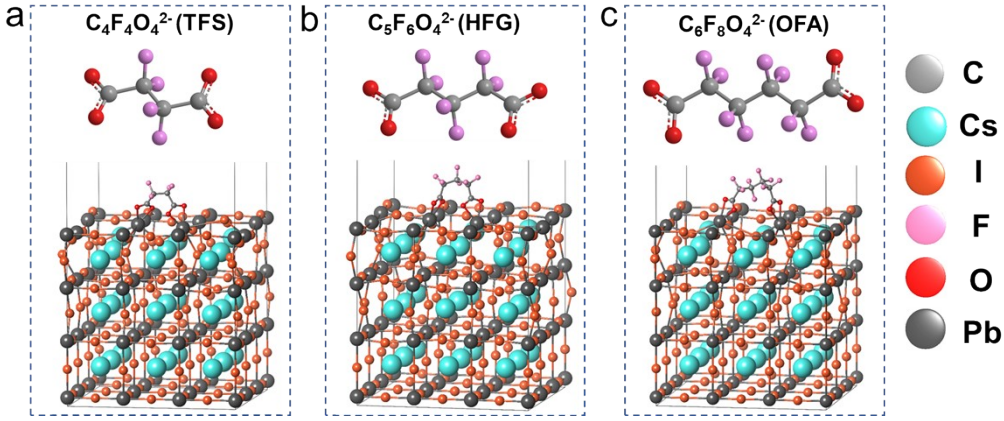

Figure S7. Atomic structure of optimized $CsPbI_3$ (001) surface with (a) TFS, (b) HFG and (c) OFA anions, respectively.

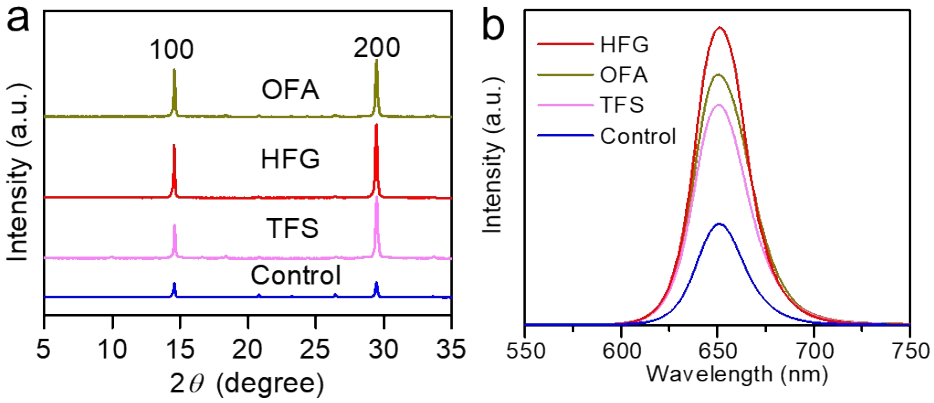

Figure S8. (a) XRD patterns and (b) PL spectra of the control, TFS, HFG and OFA films, respectively.

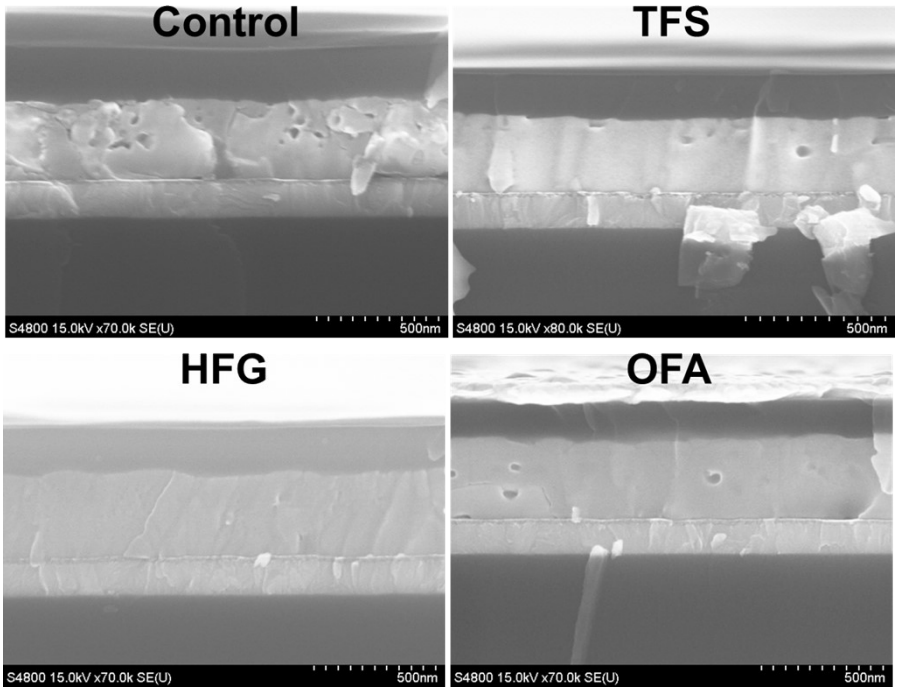

Figure S9. Cross-sectional SEM images of the control, TFS, HFG and OFA film-based PSCs, respectively.

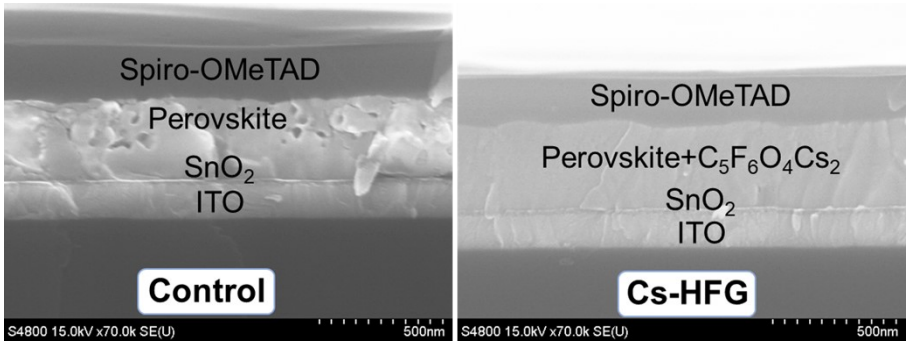

Figure S10. Cross-sectional SEM images of the control and Cs-HFG devices.

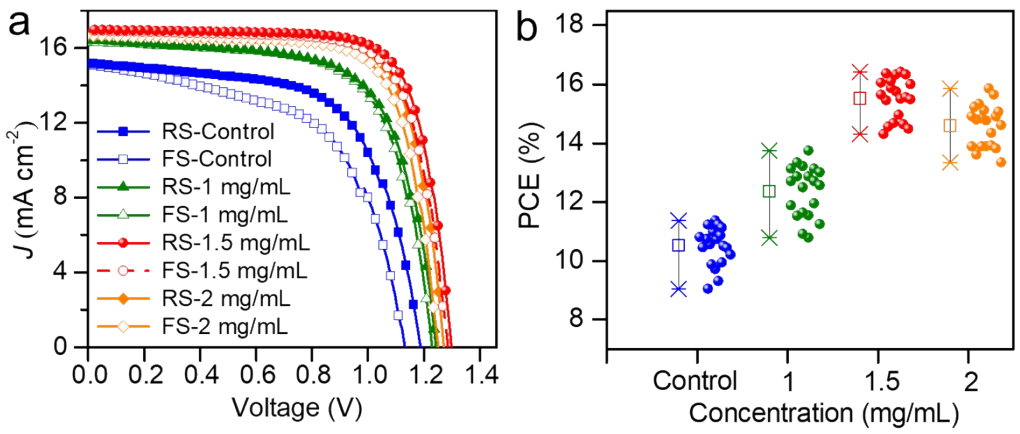

Figure S11. (a) *J-V* curves of the best performance PSCs without and with $C_5F_6O_4Cs_2$ in different concentrations and (b) distribution of 20 individual PSCs without and with $C_5F_6O_4Cs_2$ in different concentrations.

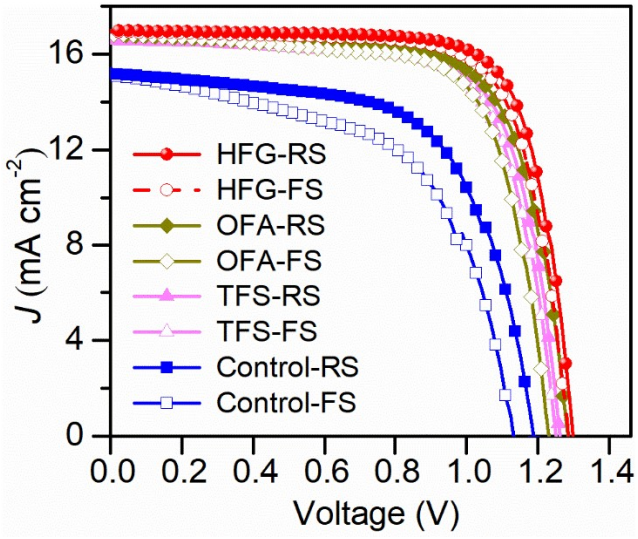

Figure S12. *J-V* characteristics of the champion devices based on control, TFS, HFG and OFA films.

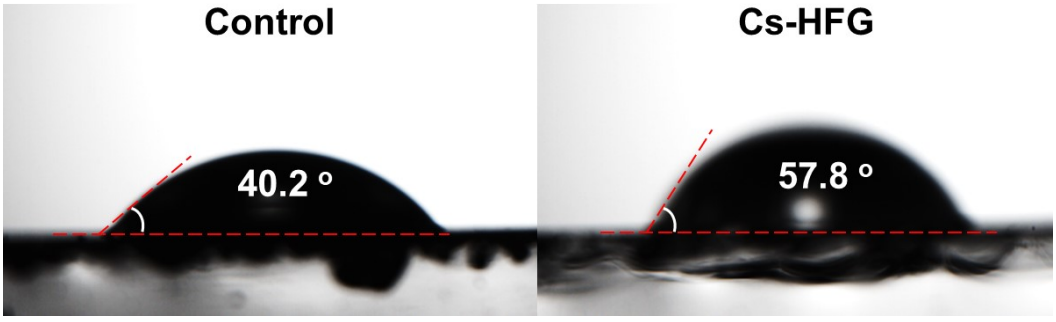

Figure S13. Water angle of the control and Cs-HFG perovskite films.

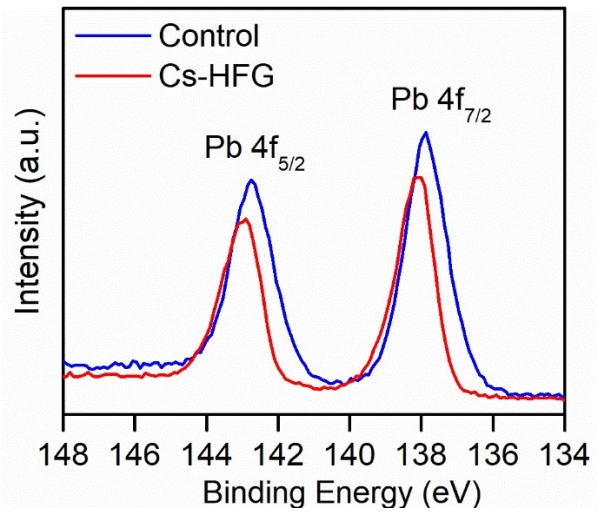

Figure S14. Pb 4f XPS spectra of the control and Cs-HFG perovskite films.

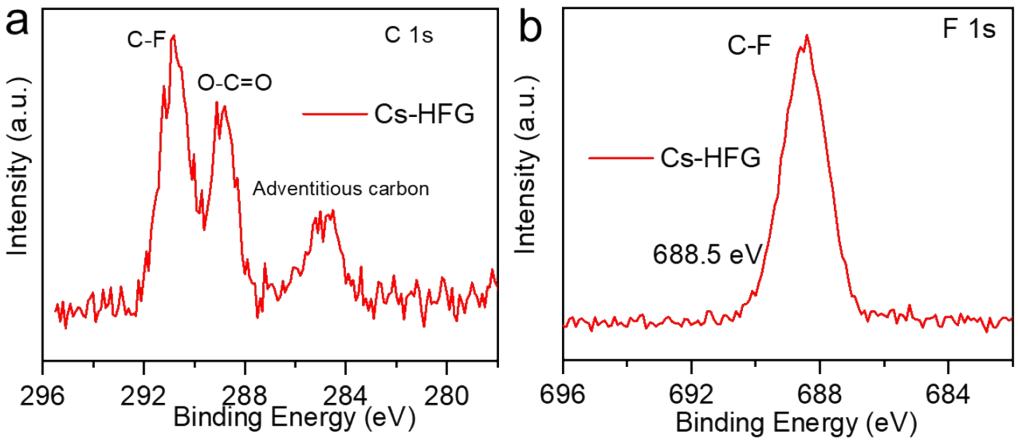

Figure S15. (a) C 1s and (b) F 1s XPS spectra of the Cs-HFG perovskite film.

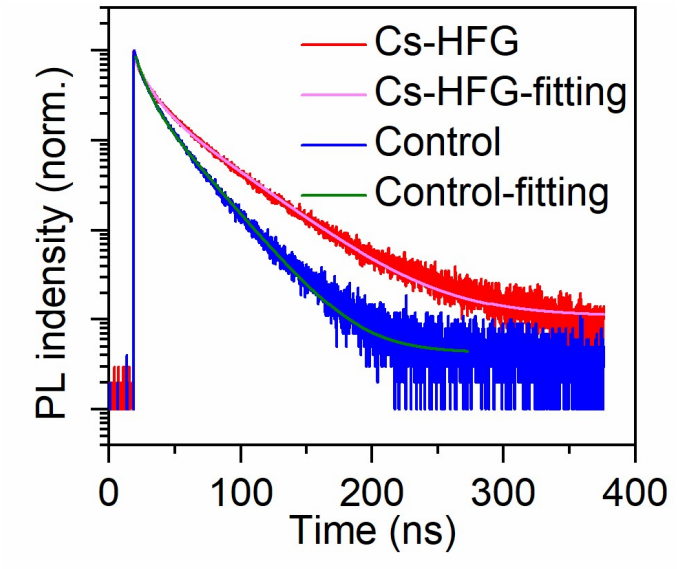

Figure S16. TRPL spectra of the control and Cs-HFG perovskite films.

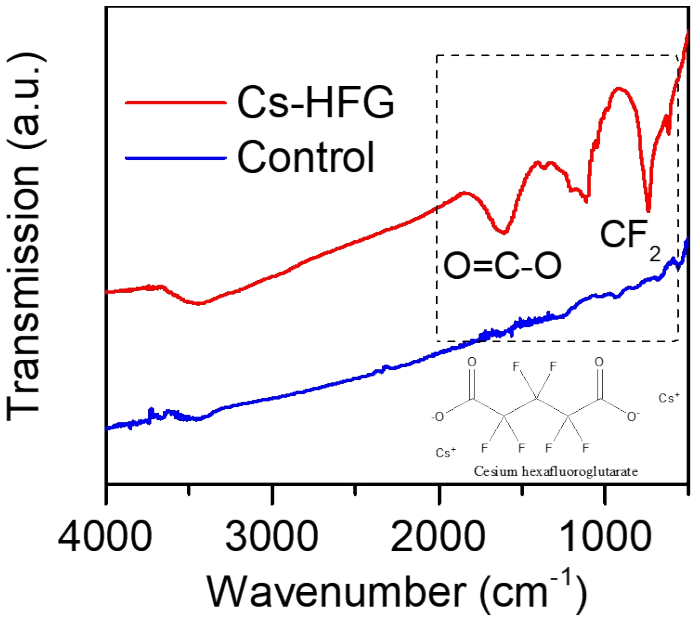

Figure S17. FTIR spectra of the control and Cs-HFG perovskite films. Inset is the molecule structure of $C_5F_6O_4Cs_2$.

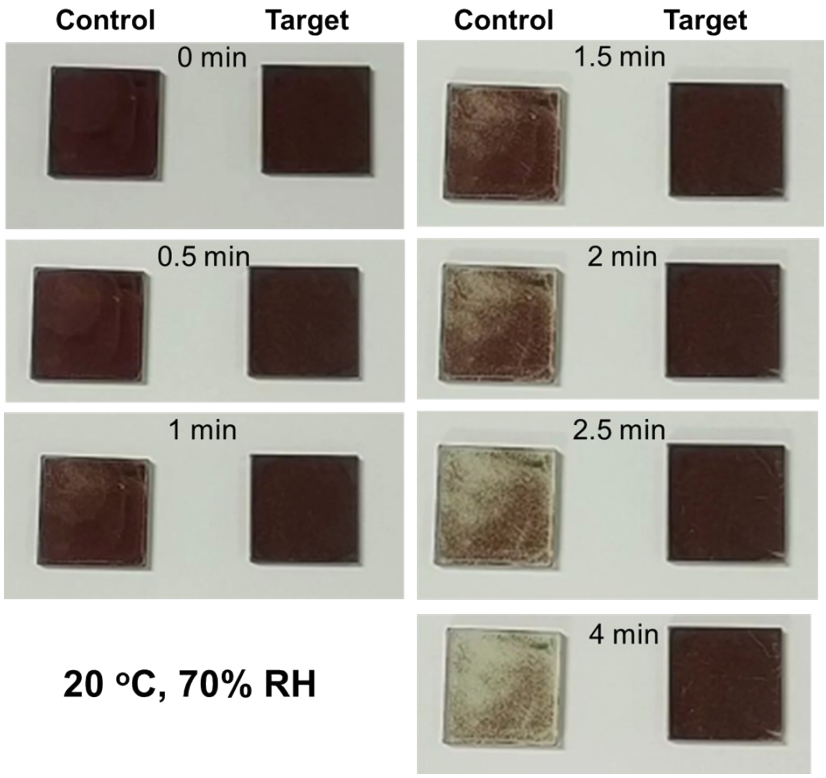

Figure S18. Digital photos of the control and Cs-HFG films (2*2 cm^2) at 20 °C and 70% RH with different aging times.

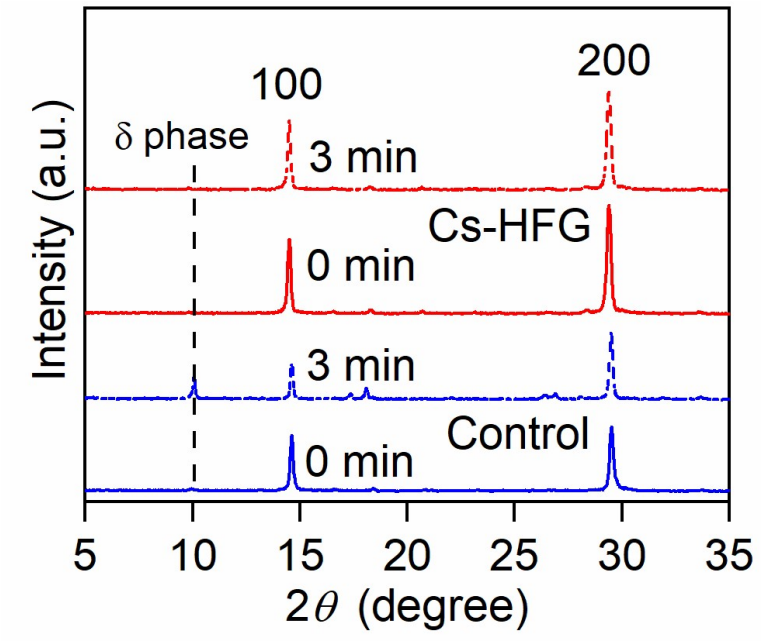

Figure S19. XRD patterns of the control and Cs-HFG films at 20 °C and 70% RH with different aging times.

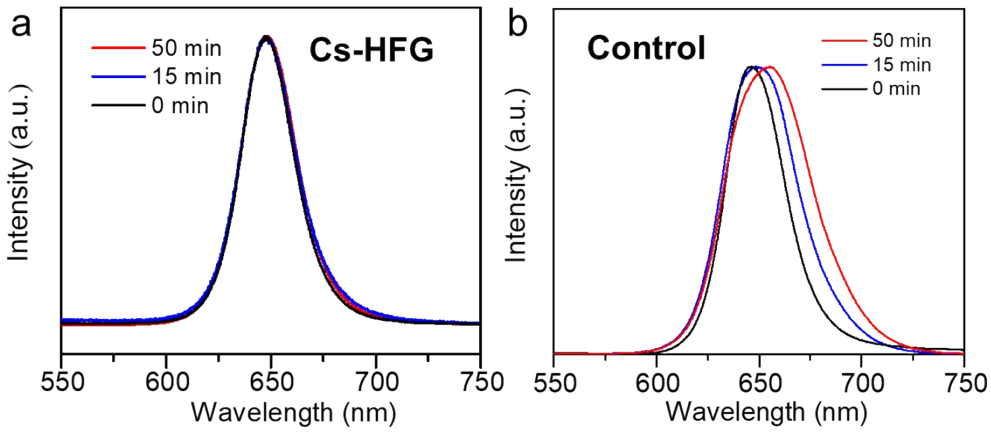

Figure S20. Normalized PL spectra of (a) Cs-HFG and (b) control films under continuous AM 1.5G illumination for 50 min. All perovskite films were deposited on glass substrates.

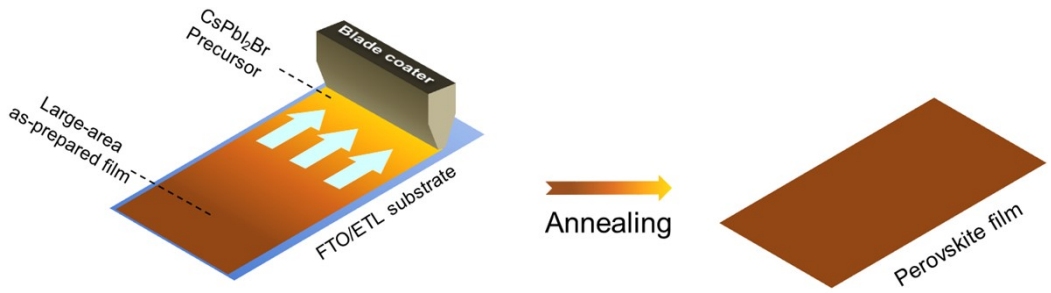

Figure S21. Schematic of the fabrication process of the large-area inorganic perovskite film by blading coating.

Table S1. Parameters of atomic structure of optimized $CsPbI_3$ (001) surface with TFS^-, HFG^- and OFA^- anions.

Anion	surface	ligand	surface+ligand	binding energy / Hartree	binding energy / eV
TFS^-	-1814.40	-183.64	-1998.29	-0.263	-7.15
HFG^-	-1814.48	-237.80	-2052.49	-0.322	-8.76
OFA^-	-1814.44	-291.98	-2106.64	-0.219	-5.96

Table S2. Photovoltaic parameters of PSCs (0.12 cm^2 of active area).

Device		J_{sc}/mA·cm^{-2}	V_{oc}/V	*FF*/%	*η*/%
Cs-HFG	Reverse	16.89	1.30	74.83	16.43
	Forward	16.86	1.28	75.6	16.31
Control	Reverse	15.17	1.19	62.93	11.36
	Forward	15.13	1.13	57.15	9.77

Table S3. Photovoltaic parameters of PSCs with different $C_5F_6O_4Cs_2$ amounts (0.12 cm^2 of active area).

Device		J_{sc}/mA·cm^{-2}	V_{oc}/V	*FF*/%	*η*/%
2 mg	Reverse	16.70	1.27	74.70	15.85
	Forward	16.65	1.25	73.21	15.24
1.5 mg	Reverse	16.89	1.30	74.83	16.43
	Forward	16.86	1.28	75.60	16.31
1 mg	Reverse	16.41	1.24	67.41	13.74
	Forward	16.32	1.23	67.69	13.57
Control	Reverse	15.17	1.19	62.93	11.36
	Forward	15.13	1.13	57.15	9.77

Table S4. Photovoltaic parameters of PSCs (0.12 cm^2 of active area) based on control, TFS, HFG and OFA films.

Device		J_{sc}/mA·cm^{-2}	V_{oc}/V	*FF*/%	*η*/%
TFS	Reverse	16.54	1.26	72.31	15.07
	Forward	16.61	1.25	70.74	14.69
HFG	Reverse	16.89	1.30	74.83	16.43
	Forward	16.86	1.28	75.60	16.31
OFA	Reverse	16.76	1.28	70.80	15.19
	Forward	16.81	1.23	70.17	14.51
Control	Reverse	15.17	1.19	62.93	11.36
	Forward	15.13	1.13	57.15	9.77

Table S5. Photovoltaic parameters of PSCs (0.12 cm^2 of active area) based P3HT as HTL.

Device		J_{sc}/mA·cm^{-2}	V_{oc}/V	*FF*/%	*η*/%
Cs-HFG	Reverse	15.09	1.25	77.26	14.57
	Forward	14.95	1.25	76.68	14.33
Control	Reverse	13.14	1.06	67.38	9.38
	Forward	13.22	1.03	48.03	6.57

Table S6. Photovoltaic parameters of the champion device of Cs-HFG PSCs (8 cm^2 of active area).

Device		J_{sc}/mA·cm^{-2}	V_{oc}/V	*FF*/%	*η*/%
Cs-HFG	Reverse	3.81	4.49	72.01	12.35
	Forward	3.76	4.52	71.03	12.07

Table S7. The performance of inorganic PSC modules by spin or blade coating in previous reports and this work.

References	Active area (cm^2)	Materials	Configuration	Perovskite preparation	PCE (%) (Reverse scan)
11	8	Crown ether	FTO/ZnO-ZnS/$CsPbI_3$/Spiro/Au	spin coating	11.87
				blade coating	10.73
12	27	CITTIN-2F	FTO/TiO_2 /$CsPbI_3$/ CITTIN-2F/Au	spin coating	11.0
13	10.92	TPFPB, $LiClO_4$	FTO/NiO_x/$CsPbI_2Br$/ ZnO@C_{60}/Ag	spin coating	12.19
This work	8	cesium hexafluoroglutarate	FTO/SnO_2 / $CsPbI_2Br$/Spiro/Au	blade coating	**12.35**

References:

[1] R. Chen, Y. Wang, S. Nie, H. Shen, Y. Hui, J. Peng, B. Wu, J. Yin, J. Li, N. Zheng, *J. Am. Chem. Soc.* **2021**, *143*, 10624-10632.

[2] R. Chen, J. Cao, Y. Wu, X. Jing, B. Wu, N. F. Zheng, *Adv. Mater. Interfaces* **2017**, *4*, 1700897.

[3] E. H. Jung, N. J. Jeon, E. Y. Park, C. S. Moon, T. J. Shin, T. Y. Yang, J. H. Noh, J. Seo, *Nature* **2019**, *567*, 511-515.

[4] R. He, S. Nie, X. Huang, Y. Wu, R. Chen, J. Yin, B. Wu, J. Li, N. Zheng, *Solar RRL* **2021**, *6*, 2100639.

[5] T. D. Kühne, M. Iannuzzi, M. Del Ben, V. V. Rybkin, P. Seewald, F. Stein, T. Laino, R. Z. Khaliullin, O. Schütt, F. Schiffmann, D. Golze, J. Wilhelm, S. Chulkov, M. H. Bani-Hashemian, V. Weber, U. Borštnik, M. Taillefumier, A. S. Jakobovits, A. Lazzaro, H. Pabst, T. Müller, R. Schade, M. Guidon, S. Andermatt, N. Holmberg, G. K. Schenter, A. Hehn, A. Bussy, F. Belleflamme, G.

Tabacchi, A. Glöß, M. Lass, I. Bethune, C. J. Mundy, C. Plessl, M. Watkins, J. VandeVondele, M. Krack, J. Hutter, *J. Chem. Phys.* **2020**, *152*, 194103.

[6] S. Goedecker, M. Teter, J. Hutter, *Phys. Rev. B* **1996**, *54*, 1703.

[7] J. VandeVondele, J. Hutter, *J. Chem. Phys.* **2007**, *127*, 114105.

[8] J. P. Perdew, K. Burke, M. Ernzerhof, *Phys. Rev. Lett.* **1996**, *77*, 3865-3868.

[9] S. Grimme, S. Ehrlich, L. Goerigk, *J. Comput. Chem.* **2011**, *32*, 1456-1465.

[10] S. Grimme, J. Antony, S. Ehrlich, H. Krieg, *J. Chem. Phys.* **2010**, *132*, 154104.

[11] R. Chen, Y. Hui, B. Wu, Y. Wang, X. Huang, Z. Xu, P. Ruan, W. Zhang, F. Cheng, W. Zhang, J. Yin, J. Li, N. Zheng, *J. Mater. Chem. A* **2020**, *8*, 9597-9606.

[12] C. Liu, C. Igci, Y. Yang, O. A. Syzgantseva, M. A. Syzgantseva, K. Rakstys, H. Kanda, N. Shibayama, B. Ding, X. Zhang, V. Jankauskas, Y. Ding, S. Dai, P. J. Dyson, M. K. Nazeeruddin, *Angew. Chem. Int. Ed.* **2021**, *60*, 20489-20497.

[13] C. Liu, Y. Yang, C. Zhang, S. Wu, L. Wei, F. Guo, G. M. Arumugam, J. Hu, X. Liu, J. Lin, R. E. I. Schropp, Y. Mai, *Adv. Mater.* **2020**, *32*, e1907361.